

Spiking Neural Networks for Visual Place Recognition via Weighted Neuronal Assignments

Somayeh Hussaini

Michael Milford

Tobias Fischer

Abstract—Spiking neural networks (SNNs) offer both compelling potential advantages, including energy efficiency and low latencies, and challenges including the non-differentiable nature of event spikes. Much of the initial research in this area has converted deep neural networks to equivalent SNNs, but this conversion approach potentially negates some of the potential advantages of SNN-based approaches developed from scratch. One promising area for high performance SNNs is template matching and image recognition. This research introduces the first high performance SNN for the Visual Place Recognition (VPR) task: given a query image, the SNN has to find the closest match out of a list of reference images. At the core of this new system is a novel assignment scheme that implements a form of ambiguity-informed salience, by up-weighting single-place-encoding neurons and down-weighting “ambiguous” neurons that respond to multiple different reference places. In a range of experiments on the challenging Oxford RobotCar and Nordland datasets, we show that our SNN achieves comparable VPR performance to state-of-the-art and classical techniques, and degrades gracefully in performance with an increasing number of reference places. Our results provide a significant milestone towards SNNs that can provide robust, energy-efficient and low latency robot localization.

I. INTRODUCTION

Spiking neural networks (SNNs) differ in several aspects from conventional artificial neural networks (ANNs) [1]. A neuron’s output within an ANN is a real number computed by a non-linear function of the sum of the inputs. This computation is different to the spikes (also called events) in SNNs, which carry a single bit of information [1]–[3]. Another difference is the learning algorithm: ANNs rely on the backpropagation of error signals, which in the standard implementation does not have an analogue in the brain [3], [4]. In contrast, the brain uses unsupervised learning methods like Spike Time Dependent Plasticity (STDP), which are also used to train SNNs [5]. Although biological insights or fidelity are not the primary focus of this paper, the premise is that SNNs are better suited to study the operation of biological systems and for (in-)validating hypotheses [1], [3].

Recently, SNNs have gained popularity in the robotics community [6]–[13], due to potential advantages over ANNs including low power consumption and low latencies. The community also has access to a growing neuromorphic hardware set, such as Intel’s Loihi [2]. SNNs have been used in disciplines including robot grasping [6], robot navigation [7], and motion planning [8]. They are however not yet widely

The authors are with the QUT Centre for Robotics, Queensland University of Technology, Brisbane, QLD 4000, Australia (e-mail: somayeh.hussaini@hdr.qut.edu.au).

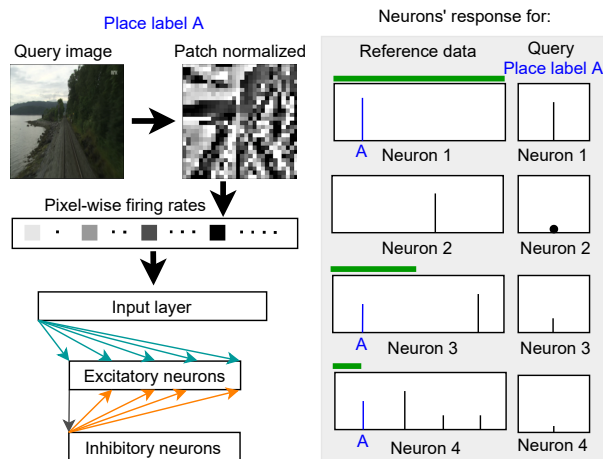


Fig. 1. A Spiking Neural Network (SNN) model for Visual Place Recognition (VPR). Left: SNN model architecture. The arrows in each layer depict the connection of one neuron to the neurons of the next layer. For simplicity, we only show the connections of a single neuron in each layer. Right: Neuronal responses to reference data and query image. We show that an ambiguity-based neuronal assignment approach that up-weights neurons that have learnt a single label and down-weights those that have learnt multiple place representations leads to significantly improved performance. In this example, the attribution of each neuron towards place label A is shown by green bars.

competitive; the resulting accuracy is generally lower compared to conventional non-spiking approaches. Current practical use (beyond scientific curiosity) is limited to narrow cases like high-speed or low power scenarios, or where closed-loop control with low latencies is required [2].

In this paper, we take a significant step towards bridging the performance divide between conventional and SNN-based techniques for the Visual Place Recognition task (VPR). VPR is critical in enabling long-term mobile robot autonomy in challenging environments: it can aid in the global re-localization of mobile robots, minimize model errors by acting as a closed-loop detection algorithm, and can be used as a component of robust localization and mapping algorithms [14]–[16].

Our research here makes the following contributions:

- 1) We introduce the first spiking neural network for the place recognition task, combining leaky integrate and fire neurons within a lightweight, biologically plausible two-layer SNN learn to represent place templates using unsupervised learning via STDP.
- 2) We introduce multiple novel neuronal assignment schemes that decode all neurons’ spike responses and weight them based on the specificity or ambiguity of a single neuron’s response to learning places.

- 3) We demonstrate competitive performance in terms of recall at 100% precision when comparing our SNN to conventional VPR baselines, namely NetVLAD [17] and the Sum-of-Absolute Differences (SAD) [18], on the Oxford RobotCar [19] and Nordland [20] datasets.
- 4) We present ablation studies showing graceful performance degradation for a fixed network size as the number of places to be learned increases.

To foster future research, we will make the code to replicate our experiments available upon acceptance.

II. RELATED WORKS

Here we review recent Spiking Neural Network research with an emphasis on robotic-related implementations in Section II-A, and an overview of related research in Visual Place Recognition in Section II-B.

A. Spiking Neural Networks

The field of neuromorphic computing concerns the development and advancement of neuromorphic hardware, sensors and associated algorithms. Diehl and Cook [21]’s two layer SNN model demonstrated the potential capability of SNN models in solving pattern recognition tasks such as digit recognition. More broadly, spiking neural networks have been evaluated in various robotics applications [6]–[13]. Head pose tracking and scene understanding tasks on the iCub humanoid robot were presented in [11]. Lele et al. [12] introduced a SNN model that receives input from an event camera for prey-tracking. Vitale et al. [13] presented a SNN to control high-speed unmanned aerial vehicles.

Biologically-inspired solutions have in particular been developed for robot navigation-related tasks including Simultaneous Localisation and Mapping (SLAM) [22]. Tang et al. [9] proposed an energy-efficient SNN model for uni-dimensional SLAM. In [23], a spiking version of place cells, grid cells and border cells of the rat hippocampus, originally proposed by [24], was implemented in neuromorphic hardware. [25] presents a SNN of place cells for 3-dimensional path planning using wavefront propagation. [10] tackled pose estimation and mapping with SNNs. Finally, [7] deployed a SNN on an autonomous robot to perform mapping and exploration of unknown environments.

While SNNs and related neuromorphic hardware have promising properties, there is often still a performance gap when compared to modern conventional learning- and algorithmic-based techniques. Due to the non-differentiable neuronal dynamics of spiking neurons, supervised techniques such as back-propagation cannot be applied in a straightforward manner. Recently, Renner et al. [26] and Lee et al. [27] proposed algorithms that approximate backpropagation, and demonstrated use on Intel’s Loihi neuromorphic hardware. Another common approach to implementing high-performing SNNs is through converting Artificial Neural Networks (ANNs) to their equivalent SNNs [28], [29]. These models can achieve comparable performance to their ANN predecessors, but may not necessarily be an ideal form of SNNs in the long term

due to not fully exploiting the advantages of computational SNNs; in particular, unsupervised methods and methods that approximate backpropagation can lead to spike-timing codes with more optimized latency and energy efficiency [2].

B. Visual Place Recognition

Visual place recognition (VPR) is the task of recognizing whether a place has been already visited given a current image of the place, and prior knowledge of previously visited places [14]–[16]. The VPR problem can be considered as a template matching problem, where the closest match of a query image is selected from a reference set of places that can be captured from significantly different viewpoint and appearance.

Early works in providing solutions to the VPR problem implemented hand-crafted feature representations – either from local points or by aggregating features over the whole image [18], [30], [31]. Many of those hand-crafted approaches have subsequently been turned into deep neural networks, enabling feature representation learning. The most popular of these approaches is arguably NetVLAD [17], based on the Vector of Locally Aggregated Descriptors (VLAD) [31], which implements a pooling layer with differentiable operations to allow end-to-end training. NetVLAD has formed the foundation for a substantial number of follow on systems [32], [33], but is still competitive performance-wise, and is used as a baseline in our experiments (Section VI-C).

One conceptually relevant method is Bayesian Selective Fusion [34], which finds the best match using *several sets of reference images*, similar to the use of multiple reference sets here to train the SNN. Other relevant work includes that of Frady et al. [35] who leverage the advantages of Intel’s neuromorphic Loihi processor [2] with a scalable k-Nearest Neighbour (kNN) searching algorithm. This work is of particular importance, as it shows that SNNs solving similar tasks to ours can achieve similar accuracy as CPU implementations, while having low latency ($\approx 3\text{ms}$) and high throughput (>300 queries/s) and low power ($\approx 10\text{W}$).

III. METHODOLOGY: PRELIMINARIES

Implementation of SNN-based models can pose a significant technical learning curve, especially for researchers coming from a conventional neural network background, so in the following sections we attempt to provide as much detail to facilitate replication (while respecting space limitations). This section introduces the SNN model by Diehl and Cook for unsupervised digit recognition [21], upon which we build our new system. The SNN contains biologically plausible mechanisms including Leaky-Integrate-and-Fire (LIF) neurons, Spike-Time Dependent Plasticity (STDP), lateral inhibition and homeostasis, which enables unsupervised learning. We follow the mathematical notations by Diehl and Cook [21].

The model consists of two layers, the input layer and the processing layer (Figure 1). The input layer converts input images into spike trains using rate coding. The input layer contains one neuron per (resized) image pixel; i.e. the number of neurons is $K_I = W \times H$, where W and H are the width

and height of the input image, respectively. The input image is converted into Poisson-distributed spike trains by using the intensity of the input pixel as a firing rate (frequency of spikes) to generate spikes in short intervals [36].

The neurons in the input layer are fully connected (all-to-all connection) to all K_P excitatory neurons in the processing layer. The processing layer also contains K_P inhibitory neurons. The k -th inhibitory neuron receives input from a single corresponding excitatory neuron k , and in turn inhibits all excitatory neurons except the one that it receives the connection from. These inhibitory connections provide lateral inhibition which enables the model to behave similar to a winner-takes-all system.

The neural dynamics for all neurons are modelled using the LIF model, which is a common representation of biological spiking neuron dynamics [8], [26], [37]. The differential equation describing the dynamics (the membrane voltage) of a LIF neuron is:

$$\tau \frac{dV}{dt} = (E_{rest} - V) + g_e(E_{exc} - V) + g_i(E_{inh} - V), \quad (1)$$

where E_{rest} is the resting membrane potential, E_{exc} and E_{inh} are the excitatory and inhibitory synapses' equilibrium potentials with associated synaptic conductances g_e and g_i .

The synaptic weights (representing synaptic strength) of the connections within the processing layer (between the excitatory and inhibitory neurons) are constant. The neuronal learning is done by adapting the synapses (connections) from the input layer to the excitatory neurons using STDP, an unsupervised biologically plausible learning method [5]. STDP models the behaviour of biological neurons where the magnitude and direction of change in synaptic strength (weight) is affected by the precise timing of presynaptic and postsynaptic spikes. Over a period of iterating over reference images in training, the synapses' weights increase the sensitivity of neurons to respond to different stimuli. In particular, all synaptic weights are modelled by the change in synaptic conductance. After a presynaptic input neuron sends a spike to the excitatory postsynaptic neuron, the synaptic connection is increased, otherwise the conductance decays exponentially. This is modelled by:

$$\tau_{ge} \frac{dg_e}{dt} = -g_e, \quad (2)$$

where the excitatory postsynaptic potential time constant is denoted by τ_{ge} . For synapses with an inhibitory presynaptic neuron, the same model is used to update conductance g_i , with inhibitory postsynaptic time constant τ_{gi} .

Neuronal learning with STDP takes place by adapting the synaptic weights between the input layer and the excitatory neurons in the processing layer. The weights are modelled using presynaptic traces x_{pre} , which are counters that record the number of presynaptic spikes. The change Δw in synaptic weights after receiving a postsynaptic spike is modelled by:

$$\Delta w = \eta(x_{pre} - x_{tar})(w_{max} - w)^\mu, \quad (3)$$

where η is the learning rate, x_{tar} is the value of the presynaptic trace when a postsynaptic spike is received, w_{max} is the maximum weight, and μ is a ratio to represent the dependence of update on previous weight.

To ensure all output neurons respond to different patterns, and that the number of spikes fired by neurons for different labels remains approximately within a limited number, a bio-inspired mechanism, homeostasis, is deployed. Homeostasis is implemented by an adaptive neuronal threshold for excitatory neurons. The inner voltage threshold to raise a spike is increased by a constant θ after a neuron fires and decreases exponentially. For details about these mechanisms, we refer the interested reader to [21] and note that our code will be made available as open-source.

IV. METHODOLOGY: NEURONAL ASSIGNMENTS

Diehl and Cook [21] considered the digit classification task, where each of the excitatory neurons unambiguously learnt to represent one of ten digits. At inference time, a ‘‘hard’’ assignment strategy was used, returning the label of the neuron that fired most to the query input (Section IV-A). As we will show in the following, this assumption (and thus the hard assignments) does not hold for the visual place recognition task. There, each place is considered as a separate class, resulting in a much larger number of places¹. As shown in Figure 1, a significant number of neurons learn to represent more than a single place (i.e. they fire to more than one place at training time). Thus Section IV-B introduces our novel *weighted* neuronal assignment strategy, taking a fine-grained account of the firing patterns at training time. Finally, Section IV-C defines a probability-based re-weighting scheme that increases the consistency between spike rates of the neural population.

A. Hard assignments

The standard neuronal assignment method as in Diehl and Cook [21], which we dub hard assignments, is implemented as follows. The excitatory neurons were assigned to place labels based on the highest average response of the neurons to a place label in all training images $r \in R$. The place label l is assigned to neuron i if the sum of all spikes at training time was the highest for that label:

$$N_i = \arg \max_l S_{i,l}^R \quad (4)$$

where N_i is the assignment of neuron i and $S_{i,l}^R$ is the total number of spikes of neuron i when given images with label l as input. We also define the set M_l that contains all neurons that are assigned to label l , i.e. $M_l = \{i \mid N_i = l\}$.

At inference time, the predicted place label l^* for a given query image q is the place label l that, summed over all neurons that were assigned to that label (i.e. $m \in M_l$), had the highest spike rate:

$$l^* = \arg \max_l \sum_{m \in M_l} S_{m,l}^q. \quad (5)$$

¹Note that we use the terms visual place recognition and place classification synonymously.

B. Weighted assignments

This section introduces our novel weighted neuronal assignment scheme. Remember that each input frame was considered as a new place, such that R images of a traverse are considered as R distinct places. With K_P excitatory neurons to distinguish between R places, we observed that the majority of these output neurons can fire spikes in response to multiple similar places at different intervals in training. Of responsive neurons, there are three groups: 1) neurons that continuously only raise spikes to one particular place label, 2) neurons that raise spikes to two labels, and 3) neurons that fire spikes for many labels. This led to our motivation for weighting the neurons according to the number of places that they have been assigned to at training time, in order to improve performance.

a) *Regularization by involvement*: The first normalization step lessens the contribution of neurons that have learnt many place labels, specifically if a neuron has learned more than $\gamma\%$ of place labels. For these neurons, the spike rate is regularized by the number of place labels that they have learned (while other neurons' spike rates are not regularized):

$$S_{i,l}^{Q'} = \begin{cases} S_{i,l}^Q & \text{if } \omega_i \leq \gamma \cdot R \\ \frac{1}{\omega_i} S_{i,l}^Q & \text{otherwise} \end{cases} \quad (6)$$

where $S_{i,l}^{Q'}$ are the regularized spike rates and $\omega_i = \text{card}(\{i \mid N_i \in M_l\})$ is the number of place labels represented by neuron i .

b) *Normalization by response strength*: The next normalization step considers how strongly neuron i has learnt label l . While the above regularization step only considered how many places a neuron has learnt, this normalization step additionally accounts for the strength of the responses; effectively measuring to what percentage label l was learnt when compared to all labels m that were learned²:

$$S_{i,l}^{Q*} = S_{i,l}^{Q'} \times \frac{S_{i,l}^R}{\sum_m S_{i,m}^R}. \quad (7)$$

c) *Penalize relevant neurons that did not spike*: The last normalization step down-weights place labels l when not all neurons $m \in M_l$ that have learned that place label fired when seeing the query image. The normalization factor is the number of spikes (at training time) of the neurons that also fired at query time over the number of spikes of all neurons that have learned this label:

$$\widehat{S}_{i,l}^Q = S_{i,l}^{Q*} \times \frac{\sum_m S_{i,m}^R \mathbb{1}_{S_{i,m}^Q > 0}}{\sum_m S_{i,m}^R}. \quad (8)$$

C. Probability-based neuronal assignments

Despite the normalization factors introduced in previous steps, the number of spikes of different query images vary across the dataset, complicating assessment of whether a place match has been made. To account for the variation in spike

numbers for different images, we converted the output spike numbers for every query image to a probability-based array. The probability-based spike numbers $\widetilde{S}_{i,l}^Q$ were achieved by min-max normalization scaled by the total number of spikes across all output neurons, as follows:

$$\widetilde{S}_{i,l}^Q = \frac{1}{\sum_k \widehat{S}_{k,l}^Q} \times \frac{\widehat{S}_{i,l}^Q - \min_k \widehat{S}_{k,l}^Q}{\max_k \widehat{S}_{k,l}^Q - \min_k \widehat{S}_{k,l}^Q}. \quad (9)$$

This method can be added as an additional step to both standard assignments and weighted assignments to increase consistency of spike rates for each neuron.

V. EXPERIMENTAL SETUP

This section presents implementation details in Section V-A, followed by the datasets and evaluation metrics used in Sections V-B and V-C respectively.

A. Implementation Details

We implemented the SNN model in Python3 using the Brian2 simulator [38] (CPU version) and BindsNET [37] (GPU version). We base our implementation on [21]. All reference and query images were resized to $W \times H = 28 \times 28$ pixels. The images were also patch-normalized [18] with patch sizes of $W \times H = 7 \times 7$ pixels to produce compact image representations.

The input images are converted from pixel values to Poisson spike trains using rate coding. In this encoding method, a firing rate is defined for each input pixel based on its intensity. The pixel intensities are scaled to cap the frequencies of input spikes to a range of 0-63.75 Hz. The $K_I = 784$ neurons in the first layer of the network each receive a spike train corresponding to the intensity of a single pixel in the input image. We used a gamma of value equal to 2% of number of labels presented in reference for the regularization term in weighted assignments. We trained the SNN model by presenting each input image for 350 ms, and defined a resting period of 150 ms to allow neuronal dynamics to decay to their initial values. For a given image, the output of the model is the number of spikes raised by the $K_P = 400$ excitatory neurons in the output layer. The model output is recorded after presenting each image. We trained the models on the reference dataset for 60 epochs.

B. Datasets

To evaluate the performance of the model, we used two widely established datasets that provide sequential images captured under different appearance conditions: Nordland [20] and Oxford RobotCar [19]. We used the same model configuration to train both datasets, and did not perform any dataset-specific fine-tuning.

The Nordland dataset [20] captures a train journey along a 728 km long route in Norway, with one traverse each in spring, summer, fall and winter. As typically done in the literature in [32], [34], [39], all tunnels, stationary periods and sections where the train travels below 15 km/h (based

²Note that most $S_{i,m}^R$ are zero.

on available GPS data) were removed. The frames have one-to-one correspondences across seasons, i.e. frame k in one season matches exactly frame k in the other seasons. We used the spring and fall traverses as the reference dataset and the summer traverse as the query dataset. To increase independence between each place label, we sampled places every 8 seconds (roughly every 100 meters) from the first quarter of data.

The Oxford RobotCar dataset [19] contains over 100 traversals around Oxford, with variations in weather conditions, times of the day and seasons and centimetre-accurate annotations. Following [34] we selected the sun and rain traverses for reference, and the dusk traverse as the query dataset³. We sampled places roughly every 10 meters.

Since the performance of different methods varies significantly depending on the particular section of the dataset that is being used [40], we performed comparisons on 15 non-overlapping sections on Nordland and 4 non-overlapping sections on Oxford RobotCar.

C. Evaluation Metrics

We use recall at 100% precision (R@100P) and area under the precision-recall curve (AUC) to evaluate the performance of the SNN model, which is consistent with many works on VPR [14], [15], [30], [34], [41]. R@100P is an important metric when using VPR to propose loop closure candidates to Simultaneous Localisation and Mapping (SLAM) systems, which ideally require maximal recall without false positives (i.e. 100% precision). AUC is a convenient summary statistic. We impose a particularly tight ground truth tolerance on our system, only considering exact matches as true matches, despite the relatively small gap between images. The top predicted place label is obtained by computing the spike rates across all sets of neurons assigned to all labels using the presented neuronal assignment methods.

VI. RESULTS

We first compare different neuronal assignment schemes on the loop closure detection task in Section VI-A. This is followed by a comparison of our method with existing approaches for VPR, namely the widely used NetVLAD [17] and Sum-of-Absolute-Differences [18], in Section VI-C. Finally, we evaluate performance for a fixed network size when increasing the number of reference images in Section VI-D.

A. Loop Closure Detection

Figure 2 and Table I present a comparison of the model performance using standard (hard), weighted, probability-based and weighted probability-based neuronal assignments on Nordland and Oxford RobotCar. Compared to hard assignments, the weighted and probability-based neuronal assignments improve the R@100P on average by 13.0% and 13.6% respectively (absolute increase). Our proposed combination of both of these methods, the weighted probability-based neuronal assignment, significantly improves the model performance on both Nordland and Oxford RobotCar datasets ($p < 0.001$; paired t -test).

³Sun: 2015-08-12-15-04-18, rain: 2015-10-29-12-18-17, dusk: 2014-11-21-16-07-03

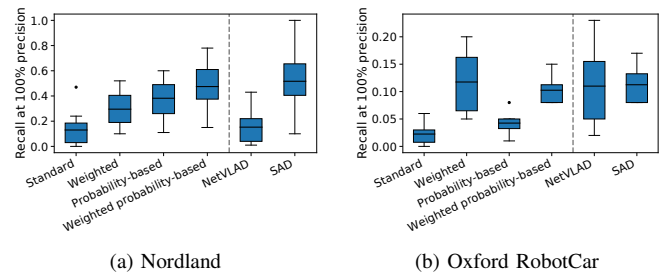


Fig. 2. Comparison of the recall at 100% precision (R@100P) for various neural assignment schemes on the Nordland and Oxford RobotCar datasets. The underlying data for the box plots stem from different sections of the dataset, where each section contains 100 places. The mean R@100P across all selected sections of dataset are indicated with a black line. For both datasets our proposed neuronal assignment schemes lead to significant improvements over the baseline.

Figure 3 shows the distance matrices of the SNN model using 100 places from the Nordland dataset, obtained by subtracting the spike rate from the maximum observed spike rate (higher spike rates indicate higher similarities). Thus lower values indicate better matches; an ideal VPR system would have low values on the diagonal and high values elsewhere. In Figure 3, the standard neuronal assignment achieved 78.0% precision at 100% recall (P@100R) and a R@100P of 2.1%. The weighted assignments increased the P@100R by 4.0% and the R@100P by 29.3%.

Figure 4 presents the SNN model performance using standard, weighted, probability-based and weighted probability-based neuronal assignments on a trial of the Nordland and Oxford RobotCar datasets. Consistent with the results presented in Figure 2 and Table I, the weighted and probability-based assignments increase recall at 100% precision compared to the standard assignments. The weighted probability-based assignments outperforms standard assignments and maintains and/or improves performance compared to weighted and probability-based assignments.

Figure 6 shows a qualitative example; in particular, the query place, the place matched by the SNN model with weighted probability-based assignment, and the corresponding reference place for the given query image. The figure also includes the templates learnt by the neurons that are assigned that place label.

B. Computational Efficiency

Table II presents the estimated inference time of the SNN model per query image on CPU, GPU and Intel’s Loihi. The SNN model presented here is simulated for each query image for 500 ms (simulated biological time, not realtime), with an update interval of 0.1 ms. This totals to 5000 timesteps per query image. The computation time per query image of the SNN model on Intel’s neuromorphic hardware, Loihi, is an estimation based on the properties of Loihi [2] and reported works of similar SNN model implementations on Loihi [35]. The estimation is done based on Intel’s Kapoho Bay USB which contains two Loihi chips and interfaces for sensor and

TABLE I

NEURONAL ASSIGNMENTS: MEAN RECALL AT 100% PRECISION FOR THE SNN MODEL FOR 15×100 PLACE TRIALS ON NORDLAND AND 4×100 PLACE TRIALS ON OXFORD ROBOTCAR, USING STANDARD, WEIGHTED, PROBABILITY-BASED, AND WEIGHTED PROBABILITY-BASED NEURONAL ASSIGNMENTS.

Datasets	Standard	Weighted	Probability-based	Weighted probability-based	NetVLAD	SAD
Nordland	13.0%	29.5%	38.2%	47.5%	15.3%	51.7%
Oxford RobotCar	2.3%	11.8%	4.3%	10.3%	11.0%	11.3%

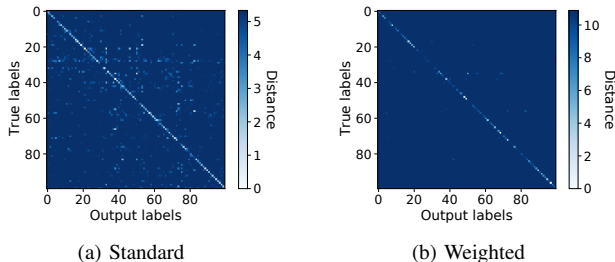


Fig. 3. Distance matrices of SNN model on a trial of Nordland with 100 places post-processed with standard and weighted neuronal assignments. The weighted assignments improve the model performance by upweighting neurons that have learnt one label and downweighting neurons that have learnt multiple labels. Compared to the standard assignments, the weighted assignments decreases aliasing and maintains and/or improves precision at 100% recall and recall at 100% precision.

event-based cameras [2]. This chip can be deployed on low-power and compact mobile robotic systems.

The CPU simulations were run on Ubuntu 20.04 with an Intel Core i7-10700K CPU @ 3.80GHz and 32Gb RAM. Based on the profiling tool of Brian2 Simulator, the processes that have the highest time requirement are synaptic weight updates to produce output spikes (average of 304 ms) and the operations for updating internal neuronal dynamics modelled by leaky integrate and fire neurons (as introduced in Section III) in excitatory and inhibitory layers (242 ms and 214 ms respectively). The estimated computation time for GPU is based on a GeForce 1080Ti GPU.

TABLE II

ESTIMATED INFERENCE TIME OF SNN MODEL ON CPU, GPU AND INTEL'S LOIHI. THE SIMULATION TIME OF EACH QUERY IMAGE IS 500 MS, 350 MS OF IMAGE PRESENTATION, AND 150 MS OF RESTING PERIOD TO ALLOW THE DECAY OF NEURAL DYNAMICS TO THEIR INITIAL VALUES.

Hardware	Inference Time per Query [s]
CPU	1.0
GPU	0.2
Intel's Loihi	< 0.05 (approximation)

C. Comparison to State-of-the-art VPR Approaches

This section provides a comparison of our proposed SNN model with standard VPR methods, namely the simplistic Sum of Absolute differences (SAD) [18] and a state-of-the-art approach, NetVLAD [17].

SAD measures the pixel-wise difference between the reference and query images. For a fair comparison, the input images of the SAD model were pre-processed with the same configuration as our SNN model (same image size and patch

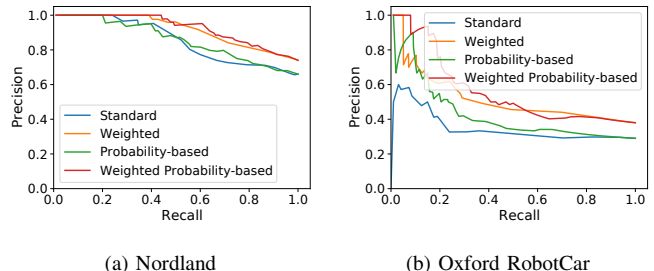


Fig. 4. Comparison of SNN model post-processed with different neuronal assignments on Nordland and Oxford RobotCar with 100 places: the weighted, and probability-based assignments can improve performance compared to the standard assignments. The combination of both approaches, weighted probability-based assignments outperforms the standard assignments.

normalization; see Section V-A). NetVLAD is known to generalize well across different datasets, having high robustness to both viewpoint and appearance changes. Due to the VGG backbone, NetVLAD requires input images to be at least 240×240 pixels, which is significantly higher than the input resolution to our SNN and SAD.

Figure 2 and Table I present a comparison of SNN model performance using standard, weighted, probability-based and weighted probability-based neuronal assignments as well as NetVLAD and SAD methods. For the Nordland dataset, the mean $R@100P$ of the SNN model with weighted probability-based assignment is comparable to the performance of SAD with an average $R@100P$ of 47.7% and 51.7% respectively. We note that the performance of NetVLAD on the Nordland dataset known to be relatively low due to the different training dataset [15], [42]. For Oxford RobotCar dataset, the mean $R@100P$ of the SNN model with weighted (11.8%) and weighted probability-based (10.3%) is comparable to that of NetVLAD (11.0%) and SAD (11.3%). The Oxford RobotCar dataset is challenging due to appearance change (sun and rain reference images and dusk queries) and occlusions.

Getting an SNN-based model to not only mechanistically perform the Visual Place Recognition task, but also achieve broadly comparable performance to SAD [18] and NetVLAD [17] represents a substantial step forward. We note however that these existing techniques have been demonstrated on larger datasets, making further scalability (beyond the studies already presented here) one of the core foci of future work with the SNN-based approach.

D. Ablation Study: Varying number of places

In this section, we analyze model performance (using our proposed weighted neuronal assignments) with a varying

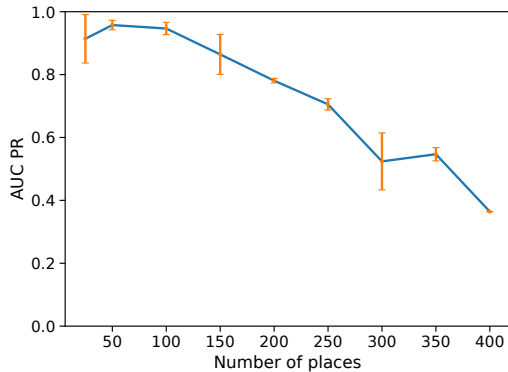


Fig. 5. SNN model performance with varying number of places (25, 100, 150, 200, 250, 300, 350, 400). With a fixed network size, the model performance degrades gracefully with increasing number of places.

number of place labels: 25, 50, 100, 150, 200, 250, 300, 350, and 400 places. The same model configuration as previously was used without any modification, except for lowering the number of epochs when increasing number of places⁴. As described in Section V-B, up to this point 15 non-overlapping sections of the Nordland dataset were used for evaluation. In this study, we instead always cover the same section of the Nordland dataset, specifically the section that covers 400 place labels. Therefore, the model learning 25 place label was repeated 16 times on consecutive sections ($16 \times 25 = 400$), the model with 50 place label was repeated 8 times, and so on. For the evaluation points where 400 is not divisible by the number of places, at least two sections were evaluated with varying offsets⁵.

Figure 5 shows that as the number of place labels increases, the performance of the model gracefully degrades when more than 100 places are learned. This is expected as the number of neurons assigned to a particular place label decreases with increasing number of places to encode, and the number of labels learnt by a neuron increases. Consequently, a single neuron outputs a higher number of spikes for *different* place labels, resulting in worse performance. In Section VII we discuss how a network with an increased number of neurons will likely lead to the ability to maintain performance as more places are encoded.

VII. CONCLUSIONS

This research demonstrated that a two-layer SNN can be adapted for the place recognition task, through the introduction of a new weighted assignment scheme, and that it could achieve comparable performance to classical and state-of-the-art techniques on benchmark robotics datasets with significant degrees of appearance change. Future work will pursue a number of promising directions. Firstly, we will investigate scaling the model size up to arbitrarily large environments, evaluating in

⁴24, 60, 60, 60, 30, 20, 20, 20 and 15 epochs for 25, 50, 100, 150, 200, 250, 300, 350, and 400 places respectively

⁵250, 150, 100 and 50 offsets for 150, 250, 300 and 350 places respectively

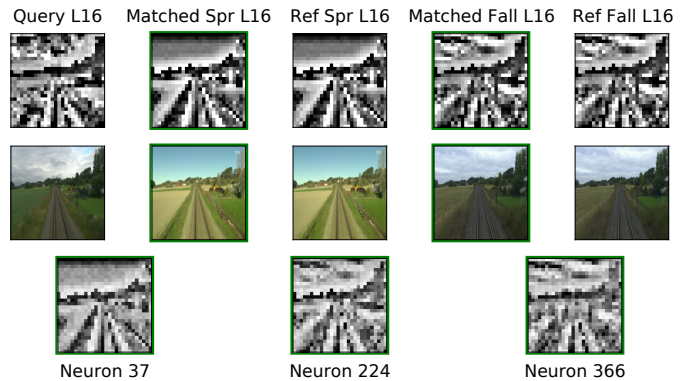


Fig. 6. Qualitative Results: An example of a query image from summer dataset correctly matched to its corresponding reference place from spring and fall traverses (indicated by green borders), in resized and patch normalized form as well as in original form. The last row shows the templates learnt by the neurons assigned to this place.

particular how training and compute requirements scale and the resulting effect on performance. We are also working with industry to deploy this system on new neuromorphic hardware including Intel’s Loihi. Such deployment has previously shown promise in terms of achieving high energy efficiencies with high throughput *and* low latencies [35]. Integrating the VPR capability into a full SNN-based SLAM system will also assist in enabling deployment of this system on low power, low cost robots, especially those with tight energy constraints. Finally, rather than converting intensity images to spike-trains, we are investigating the use of event cameras [43] that directly provide spikes as output, providing the potential for a further reduction in energy consumption and localization latency.

ACKNOWLEDGMENTS

This work received funding from the Australian Government via grant AUSMURIB000001 associated with ONR MURI grant N00014-19-1-2571, Intel Research via grant RV3.248.Fischer, and the Queensland University of Technology (QUT) through the Centre for Robotics.

REFERENCES

- [1] W. Maass, “Networks of spiking neurons: the third generation of neural network models,” *Neural networks*, vol. 10, no. 9, pp. 1659–1671, 1997.
- [2] M. Davies, A. Wild, G. Orchard, Y. Sandamirskaya, G. A. F. Guerra, P. Joshi, P. Plank, and S. R. Risbud, “Advancing neuromorphic computing with Loihi: A survey of results and outlook,” *Proceedings of the IEEE*, vol. 109, no. 5, pp. 911–934, 2021.
- [3] W. Maass, “To spike or not to spike: that is the question,” *Proceedings of the IEEE*, vol. 103, no. 12, pp. 2219–2224, 2015.
- [4] J. C. Whittington and R. Bogacz, “Theories of error back-propagation in the brain,” *Trends in Cognitive Sciences*, vol. 23, no. 3, pp. 235–250, 2019.
- [5] H. Markram, W. Gerstner, and P. J. Sjöström, “Spike-timing-dependent plasticity: a comprehensive overview,” *Frontiers in Synaptic Neuroscience*, vol. 4, no. 2, 2012.
- [6] J. C. V. Tiesck, H. Donat, J. Kaiser, I. Peric, S. Ulbrich, A. Roennau, M. Zöllner, and R. Dillmann, “Towards grasping with spiking neural networks for anthropomorphic robot hands,” in *International Conference on Artificial Neural Networks*, 2017, pp. 43–51.
- [7] G. Tang and K. P. Michmizos, “Gridbot: an autonomous robot controlled by a spiking neural network mimicking the brain’s navigational system,” in *International Conference on Neuromorphic Systems*, 2018.

- [8] J. C. V. Tieck, L. Steffen, J. Kaiser, A. Roennau, and R. Dillmann, "Controlling a robot arm for target reaching without planning using spiking neurons," in *IEEE International Conference on Cognitive Informatics & Cognitive Computing*, 2018, pp. 111–116.
- [9] G. Tang, A. Shah, and K. P. Michmizos, "Spiking neural network on neuromorphic hardware for energy-efficient unidimensional SLAM," in *IEEE/RSJ International Conference on Intelligent Robots and Systems*, 2019, pp. 4176–4181.
- [10] R. Kreiser, A. Renner, Y. Sandamirskaya, and P. Pienroj, "Pose estimation and map formation with spiking neural networks: towards neuromorphic SLAM," in *IEEE/RSJ International Conference on Intelligent Robots and Systems*, 2018, pp. 2159–2166.
- [11] R. Kreiser, V. R. Leite, B. Serhan, C. Bartolozzi, A. Glover, Y. Sandamirskaya *et al.*, "An on-chip spiking neural network for estimation of the head pose of the iCub robot," *Frontiers in Neuroscience*, vol. 14, no. 551, 2020.
- [12] A. Lele, Y. Fang, J. Ting, and A. Raychowdhury, "An end-to-end spiking neural network platform for edge robotics: From event-cameras to central pattern generation," *IEEE Transactions on Cognitive and Developmental Systems*, 2021.
- [13] A. Vitale, A. Renner, C. Nauer, D. Scaramuzza, and Y. Sandamirskaya, "Event-driven vision and control for UAVs on a neuromorphic chip," in *IEEE International Conference on Robotics and Automation*, 2021.
- [14] S. Lowry, N. Sünderhauf, P. Newman, J. J. Leonard, D. Cox, P. Corke, and M. J. Milford, "Visual place recognition: A survey," *IEEE Transactions on Robotics*, vol. 32, no. 1, pp. 1–19, 2015.
- [15] S. Garg, T. Fischer, and M. Milford, "Where Is Your Place, Visual Place Recognition?" in *International Joint Conference on Artificial Intelligence*, 2021, pp. 4416–4425.
- [16] X. Zhang, L. Wang, and Y. Su, "Visual place recognition: A survey from deep learning perspective," *Pattern Recognition*, vol. 113, p. 107760, 2021.
- [17] R. Arandjelovic, P. Gronat, A. Torii, T. Pajdla, and J. Sivic, "NetVLAD: CNN architecture for weakly supervised place recognition," *IEEE Transactions on Pattern Analysis and Machine Intelligence*, vol. 40, no. 6, pp. 1437–1451, 2018.
- [18] M. J. Milford and G. F. Wyeth, "SeqSLAM: Visual route-based navigation for sunny summer days and stormy winter nights," in *IEEE International Conference on Robotics and Automation*, 2012, pp. 1643–1649.
- [19] W. Maddern, G. Pascoe, C. Linegar, and P. Newman, "1 year, 1000 km: The Oxford RobotCar dataset," *International Journal of Robotics Research*, vol. 36, no. 1, pp. 3–15, 2017.
- [20] N. Sünderhauf, P. Neubert, and P. Protzel, "Are we there yet? Challenging SeqSLAM on a 3000 km journey across all four seasons," in *IEEE International Conference on Robotics and Automation Workshops*, 2013.
- [21] P. U. Diehl and M. Cook, "Unsupervised learning of digit recognition using spike-timing-dependent plasticity," *Frontiers in computational neuroscience*, vol. 9, 2015.
- [22] C. Cadena, L. Carlone, H. Carrillo, Y. Latif, D. Scaramuzza, J. Neira, I. Reid, and J. J. Leonard, "Past, present, and future of simultaneous localization and mapping: Toward the robust-perception age," *IEEE Transactions on Robotics*, vol. 32, no. 6, pp. 1309–1332, 2016.
- [23] F. Galluppi, J. Conradt, T. Stewart, C. Eliasmith, T. Horiuchi, J. Tapson, B. Tripp, S. Furber, and R. Etienne-Cummings, "Live demo: Spiking RatSLAM: Rat hippocampus cells in spiking neural hardware," in *IEEE Biomedical Circuits and Systems Conference*, 2012, p. 91.
- [24] M. J. Milford, G. F. Wyeth, and D. Prasser, "RatSLAM: a hippocampal model for simultaneous localization and mapping," in *IEEE International Conference on Robotics and Automation*, 2004, pp. 403–408.
- [25] L. Steffen, R. K. da Silva, S. Ulbrich, J. C. V. Tieck, A. Roennau, and R. Dillmann, "Networks of place cells for representing 3d environments and path planning," in *IEEE RAS/EMBS International Conference for Biomedical Robotics and Biomechatronics*, 2020, pp. 1158–1165.
- [26] A. Renner, F. Sheldon, A. Zlotnik, L. Tao, and A. Sornborger, "The back-propagation algorithm implemented on spiking neuromorphic hardware," *arXiv:2106.07030*, 2021.
- [27] C. Lee, S. S. Sarwar, P. Panda, G. Srinivasan, and K. Roy, "Enabling spike-based backpropagation for training deep neural network architectures," *Frontiers in Neuroscience*, vol. 14, p. 119, 2020.
- [28] B. Rueckauer, I.-A. Lungu, Y. Hu, M. Pfeiffer, and S.-C. Liu, "Conversion of continuous-valued deep networks to efficient event-driven networks for image classification," *Frontiers in Neuroscience*, vol. 11, p. 682, 2017.
- [29] C. Stöckl and W. Maass, "Optimized spiking neurons can classify images with high accuracy through temporal coding with two spikes," *Nature Machine Intelligence*, vol. 3, no. 3, pp. 230–238, 2021.
- [30] M. Cummins and P. Newman, "FAB-MAP: Probabilistic localization and mapping in the space of appearance," *The International Journal of Robotics Research*, vol. 27, no. 6, pp. 647–665, 2008.
- [31] H. Jégou, M. Douze, C. Schmid, and P. Pérez, "Aggregating local descriptors into a compact image representation," in *IEEE Conference on Computer Vision and Pattern Recognition*, 2010, pp. 3304–3311.
- [32] S. Hausler, S. Garg, M. Xu, M. Milford, and T. Fischer, "Patch-NetVLAD: Multi-scale fusion of locally-global descriptors for place recognition," in *IEEE/CVF Conference on Computer Vision and Pattern Recognition*, 2021, pp. 14 141–14 152.
- [33] J. Yu, C. Zhu, J. Zhang, Q. Huang, and D. Tao, "Spatial pyramid-enhanced netvlad with weighted triplet loss for place recognition," *IEEE transactions on neural networks and learning systems*, vol. 31, no. 2, pp. 661–674, 2019.
- [34] T. L. Molloy, T. Fischer, M. Milford, and G. N. Nair, "Intelligent reference curation for visual place recognition via Bayesian selective fusion," *IEEE Robotics and Automation Letters*, vol. 6, no. 2, pp. 588–595, 2020.
- [35] E. P. Frady, G. Orchard, D. Florey, N. Imam, R. Liu, J. Mishra, J. Tse, A. Wild, F. T. Sommer, and M. Davies, "Neuromorphic nearest neighbor search using Intel's Pohoiki Springs," in *Proceedings of the Neuro-inspired Computational Elements Workshop*, 2020.
- [36] W. Gerstner, W. M. Kistler, R. Naud, and L. Paninski, *Neuronal dynamics: From single neurons to networks and models of cognition*. Cambridge University Press, 2014.
- [37] H. Hazan, D. J. Saunders, H. Khan, D. Patel, D. T. Sanghavi, H. T. Siegelmann, and R. Kozma, "Bindsnet: A machine learning-oriented spiking neural networks library in python," *Frontiers in Neuroinformatics*, vol. 12, no. 89, 2018.
- [38] M. Stimberg, R. Brette, and D. F. Goodman, "Brian 2, an intuitive and efficient neural simulator," *Elife*, vol. 8, p. e47314, 2019.
- [39] S. Hausler, A. Jacobson, and M. Milford, "Multi-process fusion: Visual place recognition using multiple image processing methods," *IEEE Robotics and Automation Letters*, vol. 4, no. 2, pp. 1924–1931, 2019.
- [40] S. Schubert and P. Neubert, "What makes visual place recognition easy or hard?" *arXiv:2106.12671*, 2021.
- [41] M. Labbe and F. Michaud, "Appearance-based loop closure detection for online large-scale and long-term operation," *IEEE Transactions on Robotics*, vol. 29, no. 3, pp. 734–745, 2013.
- [42] M. Zaffar, S. Garg, M. Milford, J. Kooij, D. Flynn, K. McDonald-Maier, and S. Ehsan, "Vpr-bench: An open-source visual place recognition evaluation framework with quantifiable viewpoint and appearance change," *International Journal of Computer Vision*, vol. 129, p. 2136–2174, 2021.
- [43] G. Gallego *et al.*, "Event-based Vision: A Survey," *IEEE Trans. Pattern Anal. Mach. Intell.*, 2020, to appear.